RESEARCH ON SINTERED POROUS RESTRICTORS

FINAL STATUS REPORT

to

N A S A

George C. Marshall Space Flight Center

Huntsville, Alabama

from

KULITE TUNGSTEN COMPANY

Ridgefield, New Jersey

Contract No. NAS8-11413

April 20, 1965.

Table of Contents

List of Figures

List of Tables

I INTRODUCTION

A - Summary of Previous Work

Previous investigations concentrated on the development of the porous restrictor and the manufacture of restrictors with flow rates between 30 and 70 ^{cc}/min. Included in these investigations was the development and refinement of the sealing process. The practicality of producing porous restrictors was ascertained by the work performed in these initial investigations.

B - Statement of Objectives

The objective of this investigation was to further develop and refine the various manufacturing procedures performed on the tungsten rods with the object of instituting cost reduction. Attention was devoted to the following basic areas:

1. Improvement of fabrication techniques to permit higher yields, greater uniformity, and lower costs.

2. Further research in the use of spherical powder for restrictor construction, including investigations concerning the effect of vibration on structural integrity.

C. Accomplishments

The following listed objectives have been achieved by the research and development conducted during this investigation:

(a) Production of restrictors with flow rates as low as 5 - 10 ^{cc}/min or as high as 300 ^{cc}/min.

(b) Reduced and refined operating procedures into the manufacture of restrictors.

1. Reduced costs on several sintering and grinding operations.

2. Hydrostratically pressed tungsten into round bars.

3. Incorporated the use of a "double acting die" into normal production.

(c) Production of restrictors made from spherical powder.

(d) Investigated and compiled data on electron beam sealing parameters and their effect on yield and properties.

(e) Flame sprayed copper on tungsten rods as a substitute for electron beam sealing.

Suggestions for the improvement of the aforementioned developments are outlined in the chapter - "Future Work Recommendations".

II PROCESSING OF RODS

In the initial investigations, tungsten bars were produced by pressing in what is termed a "single acting" die. The single acting die set consists of a top punch which compresses the powder in a die. Among the major problems associated with this type of die set are the uneven density distribution and laminations that are prevalent in the tungsten bars. An uneven density distribution results in warpage during sintering and laminations cause an opening up of the bar during future processing steps. In both cases, the tungsten bars are no longer satisfactory material to be sealed and cut into restrictors.

A PRESSING

1. Double Acting Die

To alleviate many of the problems associated with a "single acting" die, a "double acting" die was designed and fabricated. Figure 1 illustrates the difference between the two die sets. Basically, the double acting die set is mounted on springs so that when the upper punch begins to compact the tungsten powder, the friction at the walls of the die body cause the die body to shift downward against the force of the springs. This in effect

simulates the condition of two punches (an upper and lower punch) compressing the powder in two directions as illustrated in Figure 1. The resultant density distribution in the tungsten bar is much more evenly distributed than that of the single acting die. Figure 2 is a plot of density versus distance from the movable upper punch. Note the less abrupt change in "green" density caused by pressing in a "double acting" die set. The addition of 2% paraffin as a lubricant and binder further reduces the green density distribution in the tungsten bar. Several hundred bars have been produced using the double acting die set, and have been found to be generally free of laminations or slivers. Breakage, or the ratio of broken bars to fully processed bars, have rarely exceeded 5%. The ease of loading the die and ejecting the compact in the "double acting" die set has increased the production rate twofold. A general improvement in pressing and processing has been the apparent advantage of this double acting die set.

2. Hydrostatic Pressing

Hydrostatic or isostatic pressing is the technique of compacting metal or ceramic powders in a fluid medium resulting in pressure exerted equally on all portions of the compact. The major advantages of this technique are as follows:-

1. Equal density distribution throughout the compact.
2. Ability to press, long cylindrical rods.
3. Inexpensive tooling requirements.

Several pieces were pressed on a Model 220E-10124-30 Loomis Isostatic Press produced by the Loomis Engineering & Manufacturing Company, Caldwell, New Jersey. After pressing, the rods were processed in an identical fashion as the hydraulically pressed bars. Table 1 is a compilation of the data accumulated on the hydrostatically pressed rods. The flow rates of all the bars tested tended toward 30 cc/min (those in the range of 22-25 cc/min could be easily lapped up to 30 cc/min).

Hydrostatic pressing was found to be a feasible method of producing porous restrictors. However, the major disadvantages center about economics and production rates that can be achieved by this method. The cost of purchasing a hydrostatic press would require a demand for very large quantities of restrictors which is not apparent at this date. Loading the tooling with powder, pressing and removing the compact from the tooling requires approximately five times as much time as hydraulically pressing the tungsten bars. Therefore, hydrostatic pressing cannot be economically justified at this time as a method of pressing. In other respects, hydrostatic pressing does produce bars that are round, eliminating rough grinding, requires no lubricant or binder, and results in better green density distributions than other methods of pressing.

B SINTERING and GRINDING

After completion of the pressing operation, the tungsten bars are sent through a series of debonding and sintering steps designed to cause coalescence of the tungsten particles. The degree of coalescence determines the ultimate density of the bars. Figure 3 illustrates the difference in density distributions between pressed and sintered bars. It is apparent from this graph that the sintered densities have a wider range of values than the corresponding pressed densities.

"Green" Density Range - 11.35 - 11.51 gm/cc
Sintered Density Range - 11.42 - 11.66 gm/cc

One of the means developed for compensating for the wider sintered density range is to segregate the rods into groups that fall within narrow sintered density range (e.g. 11.30 - 11.39 gm/cc; 11.40 - 11.49 gm/cc). These groups are then electron beam sealed in accordance with their density values to obtain the desired flow rate. To date, it has been possible to obtain 30 cc/min restrictors by this method; however, 55 cc/min restrictors have not been efficiently produced using compensating sealing settings.

The sintering and grinding steps have been carefully reviewed

to determine what steps could be eliminated for a more economic and productive operation. Initially, the debonding, sintering, and grinding operations were performed in the following pattern:

1. Debonding - 325°C
The function of this step is to remove all of the binder (paraffin) from the material. No sintering action takes place.

2. Presinter - 950°C
This step reduces and removes the majority of oxides remaining in the powder, This is extremely important to prevent sintering of the oxides which would result in inconsistent results. Minor sintering action occurs.

3. 1st Sinter - 1150°C
Sintering begins to take place at this temperature.

4. Rough Grinding
Round corners of bar to allow passage of rod into 0.250" diameter collet.

5. 2nd Sinter - 1420°C
Sintering begins to take place at this temperature

6. Centerless Grinding
Rod is precision ground from 0.250" diameter to 0.187" diameter.

7. Final Sinter - 1650°C
Final sintering action takes place at this temperature.

8. Centerless Grinding
Final grind from 0.187" diameter to $0.104^{+.000}_{-.001}$"

The above procedure was costly and time consuming causing great delays in processing large quantities of rods. Investigation into methods of improving the sintering and grinding operations have altered the procedure in accordance with the following outline:-

1. Debond - 325°C

2. Presinter - 950°C

3. 2nd Sinter - 1450°C

4. Rough Grinding
Instead of grinding by hand, a fixture is used which can grind 4-6 bars per set up. The bars are formed into a hexagonal shape by breaking the four corners.

5. Final Sintering - 1650°C

6. Final Grinding
The rods are now centerless ground from a hexagonal shape approximately 0.250" across the flats to $0.104^{+.000}_{-.001}$ in one operation. The intermediate grinding operation previously performed has been eliminated.

Comparison of the new method of sintering and grinding with the old method indicates that the number of operational steps has been reduced from 8 to 6. The reduction in operational steps has aided in improving the flow of bars in process, especially for large quantities. Results of density determinations on sintered rods has yielded no significant difference in the final densities achieved by the elimination of the 1st sinter (1150°C) operation.

Due to the fact that total shrinkage is in the order of 2% or less, no detrimental shrinkage cracks have been noted on any of the processed rods. In general, the new method of sintering and grinding has been found more economical and efficient with no appreciable loss in control.

C LOW FLOW RATE RESTRICTORS

In order to manufacture a low flow rate porous restrictor, it was necessary to utilize a much finer powder than used in the manufacture of 30 and 55 cc/min restrictors. Previous work had shown the relationship between particle size, density, and flow rate, and is shown in Figure 4.

Test discs were fabricated using 1.45 and 6.8 micron powder to determine the effect of sintering on the final flow rate. Table 2 is a compilation of data obtained from the test discs. Discs numbered 1, 2 and 3 had the greatest increase in density (average of 9%) in comparison to discs 4, 5 and 6 which showed no appreciable increase in density.

The relative high increase in density can be attributed to the smaller particle size (1.45 microns) for discs 1, 2 and 3. The flow rates for the 1.45 tests discs were approximately 1/5 to 1/3 slower than the corresponding test discs fabricated with 6.8 micron powder. Therefore, it was ascertained that large variations in flow rate requirements could be achieved by varying the particle size.

Bars of 1.45 micron powder were compacted in a double acting die in the exact fashion as the 6.8 micron bars.

Table 3 reports the data on four bars that were pressed and sintered with their resultant flow rates. Note that it was necessary to alter the presintering temperature (up from 950°C to 1000°C) and final sintering time (up from 2 hours to 8 hours) in order to achieve the sintered density needed to obtain 5 cc/min restrictors. Presintering at 1000°C was necessary in order to promulgate enough sintering action to prevent damage due to movement of the bars between furnaces in subsequent operations. Final sintered densities have to be approximately 70% of theoretical density.

Because of the increase in final sintered density to 70% of theoretical, shrinkage of the bars was substantially reduced during the electron beam sealing process. Therefore, the bars were centerless ground to $0.102 \pm^{.000}_{.001}$ instead of $0.104 \pm .001$. Electron beam sealing caused the bars to further shrink to 0.099 to 0.100" when sealed at 1.75 ma and 110 Kv.

Lapping and cleaning operations were essentially identical to those used in processing 6.8 micron rods. Fifty restrictors were produced and shipped in fulfillment of this contract.

It has been determined feasible to produce low flow rate restrictors efficiently without altering to any great extent any of the normal processing parameters.

D SPHERICAL POWDER AND RESTRICTORS

Further study into the feasibility of using spherical tungsten powder for porous restrictors was undertaken in this investigation. A standard distribution tungsten powder was coated with 0.05% nickel and flow rates were compared to previous data on 1.5 and 25 micron tungsten microspheres.

The particle size distribution of the standard distribution powder is graphically plotted in Figure 5. Skewness of the curve to the left indicates the majority of particles are in the range of 40 - 80 microns.

In the previous test programs 0.1% nickel was added to the tungsten. However, in this group of bars, 0.05% nickel was added to study the final sintering characteristics. The addition of nickel is predicated on the requirement of a more rigid, higher density restrictor with greater structural integrity, but the same permeable porosity as those developed in the previous programs. Spherical powder has a smaller ratio of surface area to volume than non-spherical and there is consequently a lower surface free energy available as a thermodynamic driving force for sintering. However, at the sintering temperatures used, the nickel is near or at its melting point. This greatly enhances the rate of atomic migration

both of nickel and tungsten atoms. Tungsten and nickel can form a liquid state solution with atoms of both species migrating at a rate 10^5 times more rapidly than in solid state. Sufficient tungsten will be dissolved in the nickel to achieve thermodynamic equilibrium and this dissolution will give rise to substantial densification which could not be achieved without the presence of the liquid phase. The resulting structure will in fact not be nickel coated after sintering, but will be a solid solution of nickel in tungsten, and a much more rigid structure will result. Even with the decrease in nickel content from 0.1% to 0.05%, the final sintering temperature to achieve densification was 1450 - 1500°C compared to 1650°C for the 6.8 micron standard distribution non-spherical powder.

The results of pressing, sintering and electron beam sealing the spherical tungsten powder are listed in Table 4. The sealed densities are approximately 70% of the theoretical density of tungsten and are close to 10% higher than the densities obtained after electron beam sealing 6.8 micron non-spherical powder. However, the flow rates for the standard distribution spherical powder are nearly 5 to 6 times higher than any other spherical or non-spherical powders compacted to date. Table 5 is a comparison of flow rates of all the spherical powders used in the preparation and manufacture of porous restrictors. Note that the 0.05% nickel coated standard distribution spherical powder has the highest flow rate.

With regard to spherical powders, by varying the nickel content, distribution or particle size, it is possible to obtain a wide range of flow rates.

It is interesting to note that the spherical powder yielded a much higher flow rate for a given sealed density than the 1.45 and 6.8 micron bars. Due to the particle shape and the fully dense spherical particle, more uniform sintering action was observed and consequently, the final sealing operation produced more consistent final densities. A final advantage is the better control exercised over sintering because the sintering process is liquid phase activated by the addition of nickel.

Cost appears to be one of the disadvantages associated with spherical particle powder. Where non-spherical powder costs $3.00 per pound for a standard distribution, spherical powder costs approximately $35.00 per pound. And for a given particle size distribution, spherical powder costs in the area of $140.00 per pound. Another problem yet to be fully overcome is the compacting of spherical powders. If no binder, such as paraffin, is added to the powder before pressing, a very large percentage of bars cracked upon removal from the die. With the addition of 2% paraffin, breakage of the bars was substantially

reduced during the pressing operation. Extreme care must be exercised during the debonding operation, since removal of the paraffin makes the bars very fragile. Special precautions are observed in handling after debonding and breakage has been held to a minimum.

III ELECTRON BEAM SEALING

The primary purpose of electron beam sealing the circumference of the tungsten rod is to prevent gas leakage through the circumference of the rod. The flow of gas is therefore confined to the core, which is composed of the porous tungsten matrix.

The sealing process consists of directing a stream of high velocity electrons at the rotating tungsten rod and traversing the rod with this beam. The penetration of the beam is slight, hence, only the surface layer of tungsten is melted. However, due to the amount of heat generated by the surface melting, there is some sintering action generated in the core. Table 6 is a typical computation illustrating the increase in core density after sealing the rod. Previous investigations have produced 30 - 70 ^{cc}/min restrictors using electron beam sealing parameters derived from preliminary studies. However, with the incorporation of closer tolerances on specific flow (flow rate/unit length), more knowledge of the electron beam variables had to be accumulated and used to obtain higher process yields.

One of the most basic difficulties found to exist in the electron beam sealing process is obtaining reproducible sealed densities under identical conditions. Consistancy in sealing is of vital importance in increasing yields and reducing processing costs. Therefore, the

following variables were studied to see how they affect uniformity of the sealing process. These variables in electron beam sealing are:-

A. Beam Current

B. Beam Voltage and Power Setting

C. Speed Variation

A. BEAM CURRENT

The graph in Figure 6 is a plot of beam current (milliamperes) versus sealed density (g/cc) containing data from several different receivals. Note the wide dispersion of data at beam current readings of 1.60 and 1.65 ma. The wide dispersion is more pronounced on a lot to lot basis rather than on an individual rod basis. Normally, the sintered rods are sealed in a fixture that holds eight rods. These eight rods will have measured sealed densities that will be close in value, but, compared to previous lots the sealed densities will vary considerably as indicated in Figure 6. The importance of being able to reproduce sealed densities on a lot to lot basis is more clearly illustrated in Figures 7 and 8. Figure 7 is a graph of % yield (plugs/bar) versus Sealed Density (gm/cc) for 55 ^{cc}/min restrictors. Yields vary from 7% to 100%. Figure 8 is a histogram comparing Total % Yields versus Sealed Density. This graph indicates that the greatest number of bars with any type of yield for 55 ^{cc}/min restrictors are in the range of 12.00 to 12.20 g/cc. To obtain a sealed density of 12.00 to 12.20

g/cc, reference is again made to Figure 6 where the problem of attaining the desired sealed density is graphically illustrated. Settings at 1.60 ma (at 110 Kv) produce sealed densities that range from 12.00 to 12.60 g/cc.

Figure 3 is a frequency distribution of pressed and sintered bars. Even though the sintered densities have a wider density distribution than the pressed bars, segregation of the sintered bars into narrow density groupings permit excellent control of the bars released for sealing. Therefore, variations in final sealed density can be attributed solely to the sealing process. This variation in final sealed density produces extremely poor yields resulting in exorbitant manufacturing costs.

From the evidence gathered in these investigations, there is a tendency toward achieving a high density rather than a low one; hence, it is much easier to manufacture 30 ^{cc}/min restrictors. Possible future programs might include studies of sintering larger particle size powders to increase the permeability of the compact with a resultant increase in flow rate.

B. BEAM VOLTAGE and POWER

Experiments were conducted to study the effects of varying beam voltage and current on final flow rate. The sealing parameters were adjusted to be the equivalent power value of settings of 110 Kv and 1.75 ma and 1.60 ma (or 110 Kv x 1.75 ma = 1.925 watts; 110 Kv x 1.60 ma = 1.760 watts)

Tables 7 and 8 list the results of decreased beam voltage and increased beam current on the sealed density and flow rate of the bars. There is a noted tendency toward increasing the average flow rate with increasing beam voltage in Table 7 which had an equivalent power setting of 1.925 watts. Table 8 indicates a tendency towards decreasing flow rate with an increase in beam current (power setting of 1.760 watts). The flow rates of each category (70 Kv, 90 Kv and 110 Kv) in Table 8 were observed to be higher than the corresponding restrictor categories in Table 7. This observation appears to affirm the theory that the lower the power setting the lower the sealed density.

Although electron beam sealing at lower beam voltages has been proven feasible, no apparent advantage over the present settings is evident. It is not contemplated that the lower beam voltage settings will be used in future work unless circumstances warrant such a change.

C. SPEED VARIATIONS

It was deemed desirable to study the effects of rotational and traverse speed variations on the sealed density and final flow rate. This was accomplished by doubling the rotational speed while maintaining the traverse speed, halving thetraverse speed while maintaining the rotational speed and increasing the traverse and rotational speeds.

Figures 9 and 10 are graphs illustrating the effects of varying the traverse and rotational speeds. In Figure 9, the rotational speed was increased from 18 RPM to 36 RPM; the sealed density increases significantly in value (beam current - 1.60 ma, beam voltage 110 Kv). The reason for the increase can be attributed to the electron beam concentrating on an area for a longer period of time resulting in more sintering action. Figure 10 is a comparison of two curves where the traverse speed has been varied, and the rotational speed (18 RPM) has been held constant. Where the traverse speed decreases from 1.0 IPM to 0.5 IPM, the sealed density increases; increasing the traverse speed from 1.0 IPM to 1.5 IPM, decreases the sealed density. From these graphs, it is evident that the most effective method of obtaining the minimum sealed density is to increase both the traverse (36 RPM) and rotational speeds (1.5 IPM) for a selected sintered density.

The flow rates of the test bars, which had the rotational (36 RPM) and traverse (1.5 IPM) speeds increased, were the highest of all the groups tested. This is in agreement with the fact that these bars had the lowest sealed densities.

All of the restrictors were found to have approximately the same skin thickness (.003" $\pm$ .0005). This is very unusual because

of the variation in sealing parameters from group to group. A possible explanation for this occurrence is the cooling effect caused by increased rotational and traverse speeds, especially in the case of the 36 RPM and 1.5 IPM tests, which probably prevented excessive heat transfer to the interior of the rod. With less heating of the interior of the rod, much less sintering action was promulgated and a resultant lower sealed density was obtained for these bars (36 RPM and 1.5 IPM).

IV. NEW SEALING PROCESSES

A. SUMMARY OF PREVIOUS INVESTIGATIONS

Because of the inconsistent results obtained in final flow rates when the tungsten bars were electron beam sealed, an investigation was promulgated into new possible methods of sealing the circumference of the tungsten rod. The new method of coating and the coating material had to meet the following requirements in order to be considered.

1. Non-magnetic,
2. Fully dense (no porosity),
3. Applied relatively inexpensively,
4. Non- corrosive,
5. Oxidation resistant,
6. Application must minimize heating of the core to prevent sintering action,
7. Does not alloy with tungsten.

Of the several processes investigated, the process of flame spraying appeared to meet most of the aforementioned requirements. The process equipment costs in the range of $750 - $1000 depending on the desired accessories. The use of this equipment within our own plant extends control over the process never attained in the electron beam sealing process.

Several coating materials were investigated because they had some or all of the desired attributes previously described. The

materials included zinc, nickel-chrome-boron-silicon hard facing alloy, and copper.

Zinc was initially flame sprayed onto tungsten for evaluation. The coating was observed to be brittle, oxidized and when leak tested was found to be porous. Although these results were very discouraging, future work might entail a secondary sintering operation to both remove any zinc oxides and make the coating more ductile.

The nickel-chrome-boron-silicon hard facing alloy required a special heat treatment after flame spraying to densify the coating. The heat treatment entailed heating the coating to 1800°F whereupon the coating melted. Since the tungsten core is only 50% dense, it was decided that melting the coating might cause infiltration of the coating material into the core. Also, it was later ascertained that the hard facing alloy was slightly magnetic, which is completely detrimental to the final end use. Therefore, this coating material would not be acceptable.

Copper as a coating material appeared to hold several distinct advantages in addition to those originally listed. They are:

1. The copper coating can be sintered below the sintering temperature of tungsten.

2. Sintering in a hydrogen atmosphere reduces any copper oxide formed during the flame spraying operation.

3. Copper can be used as a base material for a subsequent plating operation.

Several bars were flame sprayed with a high purity copper powder and then were sintered at 950-1000C for various periods of time. These bars were then carefully measured and the density of the sprayed and sintered coatings calculated. Table 13 shows the method of computing the skin density of the copper coating. In all cases, the coatings were only 40 to 60% dense. To verify the calculated data, a leak test was developed to indicate porosity and all of the bars tested were found to be porous. Since a porous coating is an undesirable condition, further investigation into longer sintering schedules and heavier coatings were tried in order to increase the coating density to 100%. Results of this work is described in the next section.

B. COPPER COATED TUNGSTEN RODS

1. Density and Leak Testing Results

After the initial flame sprayed bars were found to be porous, heavier copper coatings were tried in order to increase the coating density. To accomplish this and still maintain an outside diameter of $0.100 \pm .002''$, the tungsten rods had to be centerless ground to $0.091 \pm^{.000''}_{.001''}$. This would permit an approximate coating thickness of 0.010" to 0.012" to be sprayed onto the rod. Table 9 indicates the basic dimensions of the rods before spraying, after spraying and after sintering. Bars 32M, 37M, and 70 M were resintered for a

total of 3 hours to study the effect of increased sintering time on skin density. Because the initial skin densities were low, ranging from 45.0% to 63.0% of theoretical density, it was thought that an additional sintering time might increase the densification of the copper. However, only slight increases in density for bars 32M, 37M and 70M were noted (approximately 4%). To further validate the calculated determination of the skin densities, rods 32M, 70M and 72M were leak tested in a fixture as described in Figure 11. Table 10 indicates the results of the leak tests which proved all of the rods have porous skins. Bubbles were noted to be rising from the copper skin on each of the three samples tested when immersed in water under nitrogen pressure of 15 PSIG. Although these skins were porous, several possible methods of increasing the skin density have potential and should be investigated further. These methods are outlined in the section titled, "Future Work".

2. Lapping and Cleaning Procedures.

The major problem with lapping copper coated tungsten restrictors is the possibility of embedding copper into the tungsten matrix during the lapping operation. Several experiments with lapping paper, etching agents and cleaning solutions were performed to determine which technique provided a copper free tungsten matrix and cleaned the restrictor best.

Table II lists the cleaning procedure employed on restrictors 4K-6 and 4K-7. This procedure consisted primarily of using coarse grit paper, air blasts, and methyl ethyl ketone (MEK) solvent to lap and clean the restrictor. In the case of restrictor 4K-6, lapping, air blasting and cleaning continued to increase the flow rate. Restrictor 4K-7 had the same operations performed upon it, after it was lapped to a length of 0.110". It was soaked and ultrasonically cleaned in MEK and the flow rate continued to increase indicating dissolution of foreign matter in the MEK. Several other restrictors were treated in a similar fashion with the same effective results.

These tests appear to affirm the feasibility of lapping and cleaning copper coated porous tungsten without embedding copper in the tungsten matrix. With a technique developed for processing these restrictors to obtain closely controlled flow rates, the only major barrier left is a method of producing a denser copper coating.

V. NEW CUTTING AND CLEANING PROCESSES

A. NEW CUTTING PROCESSES

The present technique for slicing the electron beam sealed rods to specific lengths requires the use of a precision wafering machine. A diamond impregnated copper wheel slices the sealed rod as the table upon which the restrictors are mounted moves across the blade. The major drawback in this method of cutting is the resultant disturbed surface on the ends of the restrictor. Final lapping and cleaning procedures remove the smeared material, but these operations require meticulous care to prevent damage to the restrictor.

Investigation into other methods of cutting the restrictors resulted in the trial of Electro-Discharge Machining. EDM or spark erosion machining utilizes a graphite electrode which erodes away the tungsten rod by passing an arc between the graphite electrode and tungsten rod. The entire assembly is submerged in oil which acts as a coolant and a lubricant.

Figure 12 is a photograph of the EDM electrodes prior to the actual erosion operation. The graphite block has been machined with spaces 0.140" apart. With the present fixture, 4 restrictors at a time would be produced by spark erosion; future fixturing would permit 12 to 16 restrictors to be spark eroded at one time. Due to the properties of the graphite, for every one part of the graphite that was eroded away, 8 parts of tungsten were removed.

One of the major advantages of electro-discharge machining is the elimination of further lapping operations if the restrictor is cut to the proper length. Since there is no movement of a blade across the restrictor face, there is practically no displacement of tungsten particles during the EDM process. Careful observation of several plugs did not reveal any disturbed material on the faces of the restrictors.

Due to necessity of maintaining a coolant around the subject material during the erosion operation, the restrictor becomes saturated with the coolant oil. The removal of this oil from the internal pores of the restrictor becomes an involved procedure, requiring special care. In addition, a cost comparison of EDM versus the present method, indicates that EDM is approximately twice as costly. Therefore, it is apparent that EDM cutting is not economically or technically advantageous to pursue in greater detail. Large production quantites might alter this situation since the cost of spark erosion machining would be reduced to a competitive level with our present method.

B. NEW CLEANING PROCEDURES

Further refinements have been incorporated into the cleaning procedure to insure a more uniform and cleaner restrictor.

A completely new fixturing device , as described in Figure 13, is being used to lap the restrictors. This fixture permits the

operator to maintain a perpendicularity between the restrictor face and side which does not exceed 0.003". Closer control can also be maintained on the length of the restrictor by carefully screwing down on the adjustment screw. Several hundred plugs have been produced using this fixture with excellent results.

The cleaning procedure has been modified and revised in several instances to improve the quality of the product while at the same time increasing the rate of production. The procedure follows the outline in Table 12.

Several important innovations have been incorporated into this cleaning procedure specifically for the purpose of maintaining rigid quality to permit reproducibility of flow rates. In Step 1, the restrictors are removed from the mounting block after initially soaking in methyl alcohol. This soaking loosens the plugs and dissolves most of the excess glue. Several intermediate soakings in methyl alcohol are then performed individually on the plugs. After lapping (Step 2), the restrictors are individually soaked in distilled water to aid in removing any residue picked up during the lapping operation from the silicon carbide paper. The distilled water is removed from the cup and methyl alcohol is added (Step 4). The restrictor is soaked in methyl alcohol for 2 to 5 minutes and then the aluminum cup is placed into the ultrasonic cleaner for a minimum of 30 seconds (Step 5). After completion of Step 5, the methyl alcohol

is poured out of the aluminum cup, and the cup is placed on a hot plate at 250°F to drive off any liquids entrapped in the internal pores of the restrictor (Step 6). The restrictor is now ready for flow testing (Step 7).

Microscopic examination of restrictors prior to shipment did not disclose any residue or foreign matter on the faces of the plugs. This procedure for cleaning the porous restrictors has appeared to improve the quality of the final product.

VI PERMEABILITY ANALYSIS AND CONTROL

The Control of flow rates through porous restrictors is predicated on the ability to control the following variables:

1. Total Pore Volume
2. Average Pore Size
3. Fraction of Interconnected Pores
4. Particle Size and Shape

A large body of information has been obtained on the effect of such process parameters as selection of powder material, pressing, sintering and sealing operations on the above variables. This information may be best illustrated with reference to Figure 4 where flow permeability (flow rate/unit area/unit length) is plotted versus sample porosity, for various particle sizes and shapes.

From this figure, it can be seen that by changing the process parameters, restrictors can be manufactured with flow rates controllably varied over a two order of magnitude range.

Three trends are obvious from the data shown:

1. For one powder type, the greater the porosity, the greater the flow rate.

2. For the same particle size, a restrictor produced with spherical powder will have a greater permeability than a restrictor produced with non-spherical powder; hence, a greater fraction of interconnected pores are available with the spherical powder.

3. For the same porosity, a powder of larger particle size will have a greater flow rate; hence, a greater number of interconnected pores.

These results are in accord with the following model of the pressing and sintering operation. If one were to separately stack 60 micron and 1.5 micron spheres, the 60 micron spheres would have larger pore spaces between the spheres. Sintering would cause coalescence of the spherical particles, but the smaller particles would have a tendency toward blockage of the pore spaces, since less pore space between particles is initially available. Therefore, even though the pore volume after sintering is identical for both particle sizes, more closures or blockages would be promulgated during sintering the fine particles, hence a lower flow rate for the 1.5 micron spherical powder.

The same analysis can also be applied to the non-spherical particles, which behave in an identical manner as the spherical powders with respect to flow rate and particle size.

As stated in Item 2 at the beginning of this section, spherical powders of the same average particle size as non-spherical powders will have higher permeabilities. This is more clearly illustrated in Figure 4, where comparison of the 1.5 micron spherical and non-spherical powders, indicates a higher permeability for the spherical powder at all porosities. Models of the spherical and non-spherical particles, after compacting would show the non-spherical particles, due to their random shape, to have smaller pore openings. Because

of the smaller pore spaces, closures would be more prevalent in the non-spherical powders; hence, the reason the lower flow rate when compared to spherical powders of the same particle size.

In order to improve the yields of a given flow rate, it is proposed that future work include the establishment and use of a pore size test to control the pore size for each required flow rate. A suggested test for the calculation of pore size is the Bubble Test which would permit the calculation of the following parameters:

1. Maximum Pore Size
2. The Average Pore Size

The Bubble Test method involves the determination of the pressure necessary to force out of the filter pores a liquid which wets it completely. This pressure, called the Bubble Pressure, is determined by the shape of the particle hole, its size and the surface tension of the liquid. The following equation would permit the calculation of the maximum pore size and the average pore size:

$$R = KS/P$$

where

R is the radius of the pore.
S is the surface tension of the liquid.
P is the pressure necessary to blow bubbles through a test section of the porous metal.
K is a constant depending on the units used to measure S and P.

The first bubble to rise from the sample would indicate the maximum Pore Size, while the "boil point", or the point where individual bubbles are lost, would indicate the Average Pore Size.

It is felt that this test would provide more valuable data in determining final flow rates and development of this test under a future work program is highly recommended. The observation of the shape and distribution of bubbles during this test may also indicate the characteristics of flow when the restrictor is used in an air-bearing gyroscope assembly.

VII VIBRATION TESTS

Three different groups of restrictors were vibration tested in a special jig designed for this purpose. The jig is composed of three heavy gage aluminum plates which are bolted together during the test. The first plate serves as an air source; the second, a sample holder, and the third, to retain the millipore paper against which any loose particles may impinge. The samples themselves are inserted in the middle plate in retaining wells, and held in place using Armstrong A-2 epoxy cement. This insures no relative motion of the sample with respect to the jig and eliminates any possibility of contamination by portions of either the plugs or jig being abraded during the tests.

The vibration tests were run in the Environmental Test Laboratory of the Kearfott Division of General Precision Aerospace, 1150 McBride Avenue, Little Falls, New Jersey. The jig was loaded three separate times with either 12 copper coated (flame sprayed) tungsten restrictors, 12 6.8 micron restrictors, or 12 spherical (60 micron) tungsten restrictors and pressurized to 15 PSIG with nitrogen. The jig was then bolted onto a C25H VIBRATOR manufactured by M. B. Manufacturers and subjected to vibration from 30 to 2000 cps at a level of 10 G for one sweep (30-2000-30) in one axes for a period of one hour.

Two sweeps were performed on each test for a total test time of two hours per jig. Figure 14 is a photograph of the vibration fixture and testing equipment.

After the vibration test is completed, the entire jig assembly was brought to Ledoux & Company, 359 Alfred Avenue, Teaneck, New Jersey, Analytic Chemists, and disassembled under clean conditions taking care not to dislodge any particles, should they be present. A blank piece of millipore filter, together with the sample millipore filters were analyzed for the presence of tungsten. Table 14 reports the findings of Ledoux & Company on the analysis of the filter papers and blank. Only a trace presence of tungsten was noted on the blank and sample filter papers. It is recommended that in the future, vibration tests continually be performed on any restrictors that are subjected to different processing parameters or produced by other methods. These tests will insure that the structural integrity of the porous tungsten restrictors are maintained at the highest level.

VIII FUTURE WORK RECOMMENDATIONS

Research and development work performed in this contract have disclosed several new areas of investigation for efficiently and economically producing 30 ^{cc}/min and 55 ^{cc}/min restrictors. Below is listed categorically, future work that can be performed to improve the manufacture and production of restrictors.

1. Flame Sprayed Tungsten Restrictors

   (a) Improve coating techniques
   (b) Improve sintering techniques
   (c) Plating to achieve 100% skin density
   (d) Experiment with flame spraying lead, zinc or silicon coatings
   (e) Structural Integrity of Flame Sprayed Restrictors.

2. Production of 55 ^{cc}/min Restrictors

   (a) Use of 10 micron powder
   (b) Increased traverse and rotational speed in electron beam sealing to produce 55 ^{cc}/min restrictors.

3. Manufacture of Miniature Restrictors

   (a) Experiment in cutting restrictors less than 0.050" in length
   (b) Develop lapping and cleaning techniques for miniature restrictors.
   (c) Flow test several groups of restrictors.

4. Spherical Powders

   (a) Experiment in developing spherical restrictors with laminar flow properties
   (b) Produce spherical particle restrictors to given flow rates (30 or 55 ^{cc}/min).

5. Bubble Test

   (a) Determine Maximum Pore Size and Average Pore Size.

Table 1

HYDROSTATIC PRESSING

Bar No.	Pressure PSI	Paraffin	Green Density g/cc	Sintered Density g/cc	Sealed Density g/cc	Average Flow Rate cc/min	Electron Beam Parameters KV	MA
HIA	30,000	2%	11.71	11.97	12.42	27.0	110	1.65
HIB	30,000	2%	11.71	12.01	12.31	27.5	110	1.65
H2A	25,000	2%	11.64	11.76	12.14	30.0	110	1.65
H2B	25,000	2%	11.64	11.75	12.25	27.0	110	1.65
H3A	30,000	--	11.41	12.06	12,35	25.0	110	1.65
H3B	30,000	--	11.56	12.09	12.41	22.5	110	1.65
H4	25,000	--	11.35	11.72	12.31	25.0	110	1.65

Table 2

Low Flow Rate Restrictors

Disc No.	u	Pressure	Green Density % Theoretical	Sintered Density[x] % Theoretical	% Increase	Flow Rate cc/min
1	1.45	30,000 p.s.i.	49.64	55.00	9.77	16.0
2	1.45	30,000	50.55	55.26	8.53	15.5
3	1.45	30,000	49.78	54.95	9.43	14.5
4	6.8	30,000	56.86	57.44	+0.01	35.6
5	6.8	30,000	57.31	57.08	-0.005	44.4
6	6.8	30,000	57.09	57.44	+0.006	57.1

x Sintered in accordance with the following schedule:

Debonded	650 F
Preheated	950 C
Final Sinter	1650 C for 2 hours

Table 3

Low Flow Rate Restrictors

1.45 u Powder

Restrictor No.	Sintered (1) Density g/cc	Sealed (2) Density g/cc	% Theoretical	Flow Rate cc/min
2L	13.00	13.40	69.4	6.1
5L	13.42	13.91	72.1	4.5
7L	13.05	13.48	69.8	5.5
15L	13.02	13.43	69.6	5.7

(1) Sintered at the following schedule

(a) Debond 325°C
(b) Pre-sinter 1000C - 1/2 Hours
(c) First Sinter 1450C - 1 hour
(d) Final sinter 1650C - 8 hours

(2) Sealed using the following electron beam sealing parameters:

1.75 ma
110 Kv

Table 4

Spherical Powder

Bar No.	Corrected Green Density	Sintered Density (A)	Sealed Density	Average Flow Rate
2F	12.95 g/cc	12.40 g/cc	13.25 g/cc	295 cc/min
3F	12.95	12.36	13.36	335 cc/min
4F	12.96	12.45	13.46	280 cc/min
6F	12.96	12.54	13.39	275 cc/min

(A) Sintering Schedule

(1) Debond 650 F

(2) Pre-sinter 1050 C for 1/2 hour

(3) First sinter 1250 C for 1/2 hour

(4) Final Sinter 1450 C for 1 hour

Table 5

Particle Size and Flow Rate Comparison

Spherical Powder	Density g/cc	Flow Rate cc/min
Standard Distribution .05% Ni Coated	13.3	Approx. 300
1.5 Micron Non-Coated	12.2	Approx. 15
1.5 Micron 0.1% Ni Coated	16.7	Approx. 10
25 Micron 0.1% Ni Coated	14.8	Approx. 100

TABLE 6

COMPUTATION OF CORE DENSITY OF A SEALED BAR

The volume of a cylinder is:

$$V_r = \pi R_2^2 L$$

Using differentiation -

$$dV_r = 2\pi L R_2 dR$$

In the limit: $\Delta V_r = 2\pi L R_2 \Delta R$ (1)
where $\Delta R = R_2 - R_1$

Wt = total weight = 3.92 g
Wc = core weight
W_r = skin weight
R_2 = outside diameter = 0.050" maximum, 0.049" average
R_1 = core diameter = 0.048"
L = length of bar = 2.41 in.
ρ_R = density of skin = 19.3 g/cc
ρ_c = density of core
ΔV_r = volume of skin
Vc = volume of core

Since $W_r + W_c = Wt$; $19.3\ V_c + \rho_c V_c = Wt$

$$\therefore \rho_c = \frac{Wt - 19.3 \Delta V_r}{V_c} \quad (2)$$

From Eq. (1); $V_r = 2\pi (2.54\ cm/in)^3 \times 0.049\ in \times (0.050 - 0.048) = 2.41 \times 10^{-2} cc$

and $V_c = \pi R_1^2 L = 3.14\ (0.048)^2\ (2.54)^3 \times 2.41 = 28.6 \times 10^{-2} cc$

Eq. (2); $\rho_c = \frac{3.92 g - 19.3 \times 2.41 \times 10^{-2}}{28.6 \times 10^{-2}} = 12.05\ g/cc$

Measured Sintered Density =	11.45 g/cc
Calculated Core Density =	12.05 g/cc
Measured Sealed Density =	12.45 g/cc

Table 7

Bar No.	KV	MA	Power Watts	Sealed Density g/cc	Average Flow Rate cc/min	Skin Thickness inches
						.003
14J	70	2.75	1.925	12.6	27.5	.003
						.003
15J	70	2.75	1.925	12.3	28.5	.003
						.003
16J	70	2.75	1.925	12.3	30.0	.003
						.003
17J	70	2.75	1.925	12.6	27.0	.002
						.005
3G	90	2.15	1.925	12.2	28.0	.003
5G	90	2.15	1.925	12.2	30.0	.003
						.004
						.003
12J	90	2.15	1.925	12.3	33.0	.003
						.004
13J	90	2.15	1.025	12.3	36.0	.003
						.003
36	110	1.75	1.925	12.6	31.0	.003
						.004
55	110	1.75	1.925	12.7	46.0	.004

Table 8

Bar No.	KV	MA	Power Watts	Sealed Density g/cc	Average Flow Rate cc/min	Skin Thickness inches
26A	70	2.55	1.76	12.0	55.0	---
						.002
28A	70	2.55	1.76	12.2	38.0	.002
						.002
1C	70	2.55	1.76	12.3	31.0	.002
						.002
3J	70	2.55	1.76	12.2	34.5	.002
						.003
2J	90	1.95	1.76	12.5	31.0	.002
						.002
5J	90	1.95	1.76	12.4	31.0	.003
						.002
7J	90	1.95	1.76	12.5	26.0	.003
						.002
8J	90	1.95	1.76	12.4	33.0	.003
						.002
4B	110	1.60	1.76	12.4	46	.002
						.002
8B	110	1.60	1.76	12.4	55	.001
						.002
19B	110	1.60	1.76	12.4	45	.002
						.002
29B	110	1.60	1.76	12.5	55	.002

Table 9

Copper Coated Tungsten Rods

Bar No.	Core Diameter in.	Core Length in.	Core Volume $in.^3$	Core Density g/cc	Skin Thickness in.	Skin Weight grams	Skin % Shrinkage After Sintering[1]	Skin Density % Theoretical
H-5-B	0.0900	1.905	0.01212	11.42	0.013	0.2535	0.75	53.0
32M	0.0905	2.4506	0.01561	11.75	0.009	0.2009	0.60	45.0
37M	0.0903	2.4518	0.01570	11.76	0.009	0.2166	0.55	49.0
70	0.0899	2.4788	0.01575	11.31	0.008	0.2161	0.76	58.0
72	0.0900	2.4788	0.01577	11.34	0.014	0.4113	1.0%	58.5
75	0.0901	2.4770	0.01581	11.39	0.018	0.4904	1.8%	63.0
32M[2]							1.20	49.0
37M[2]							1.15	53.0
70M[2]							0.95	60.5

1. Sintered at 1000°C for 1 hour

2. Sintered for an additonal 2 hours (or total of 3 hours) at 1000°C

Table 10

Rod No.	Nitrogen Pressure	Particle Size	Remark[1]
32M[2]	15 PSIG	6.8	Leaks detected, coating porous
70M[2]	15 PSIG	6.8	Leaks detected, coating porous
72M[3]	15 PSIG	6.8	Leaks detected, coating porous

1 - Sample immersed in water

2 - Rods sintered for total of 3 hours

3 - Rod sintered for total of 1 hour

Table 11

Lapping and Cleaning Experiment

Restrictor No.	History	Flow Rate cc/min.	Final Length inches	Remarks
4K-6	Lapped (120 grit,) cleaned by using air blast from 90 PSIG air line, flow tested	17.0	0.131	no etchant used, no copper embedded in tungsten matrix
4K-6	Lapped (120 grit), cleaned using air pressure, flow tested	22.4	0.117	no etchant used, increase in flow rate is appreciable
4K-7	Lapped (120 grit), cleaned using air pressure, flow tested	13.5	0.161	no etchant used, no copper embedded in tungsten matrix
4K-7	Lapped (120 grit), cleaned using air pressure, flow tested	19.3	0.110	no etchant used, increase in flow rate is appreciable
4K-7	Soaked and ultrasonically cleaned in MEK, air blasted and dried	20.3	0.110	Flow rate increased

Table 12

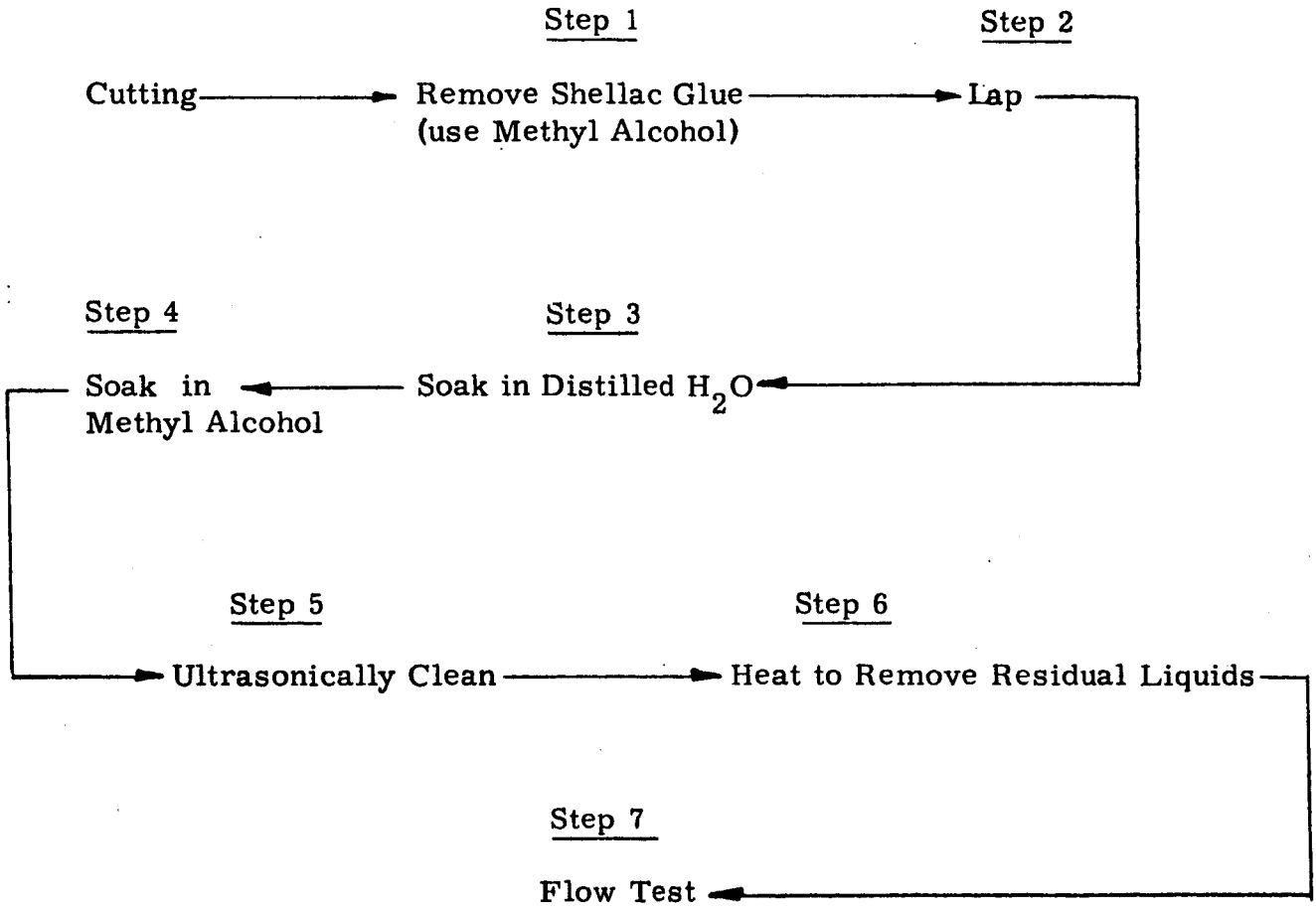
Step 1
Step 2
Cutting
Remove Shellac Glue (use Methyl Alcohol)
Lap
Step 4
Step 3
Soak in Methyl Alcohol
Soak in Distilled H_2O
Step 5
Step 6
Ultrasonically Clean
Heat to Remove Residual Liquids
Step 7
Flow Test

Table 13

Calculation of Skin Density of Copper Coated Restrictors

	Tungsten Rod	Copper Coated Rod
Diameter:	0.1044"	0.0023"
Length;	2.2245"	2.2245"
Weight:	3.520 g	3.749 g

Using the equation:

$$V_s = (V_1 + V_2)(V_1 - V_2) \times L \quad (1)$$

where V_s = Volume of skin
V_1 = Outside radius (.1123/2)
V_2 = Inside radius (.1044/2)
L^2 = Length of Rod

(1) $V_s = (.0562 + .0522)(.0562 - .0522) \times 2.2245$

$$V_s = 0.050 \text{ cc}$$

$$\text{Density of Skin} = \frac{0.229}{0.050} = 4.60 \text{ g/cc}$$

$$\% \text{ Theoretical} = \frac{4.60}{8.9} = 51.75\%$$

Table 14

Blank	Trace
6.8 Powder	Trace
Copper Coated Tungsten Powder	Trace
Spherical Powder	Trace

Analysis performed photometrically to determine quantity of tungsten present in filter paper.

DRAWING				
REVISIONS				
SYM	WAS	DATE	BY	APP

SINGLE ACTION DIE

DOUBLE ACTING DIE

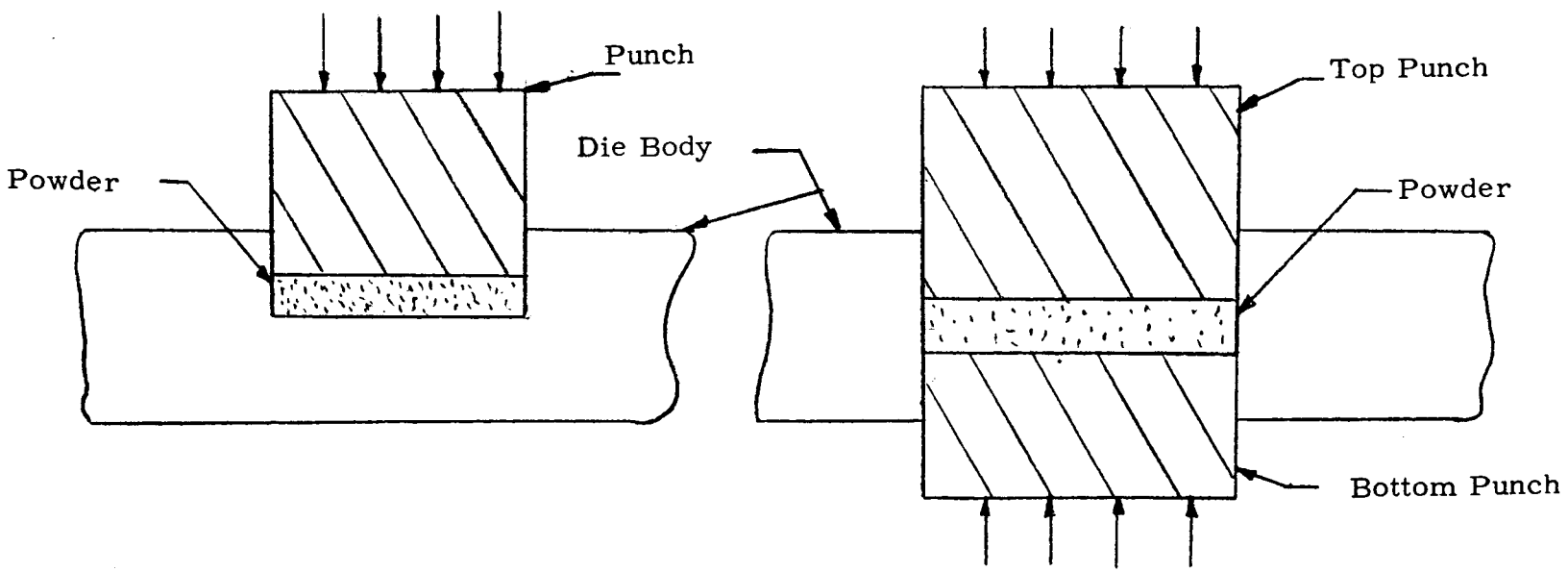

Figure 1

Description

Single and Double Acting Die Sets

UNLESS OTHERWISE SPECIFIED, TOLERANCES ON FRACTIONS ± 1/64 ON DECIMALS ± .005		DESCRIPTION	MATERIAL	KULITE TUNGSTEN CO. RIDGEFIELD, N. J.
DRAWN	CHECKED			
DATE	SCALE			

OGILVIE PRESS, INC., BROOKLYN 17, N. Y. ULTRAVEL NO. 490M

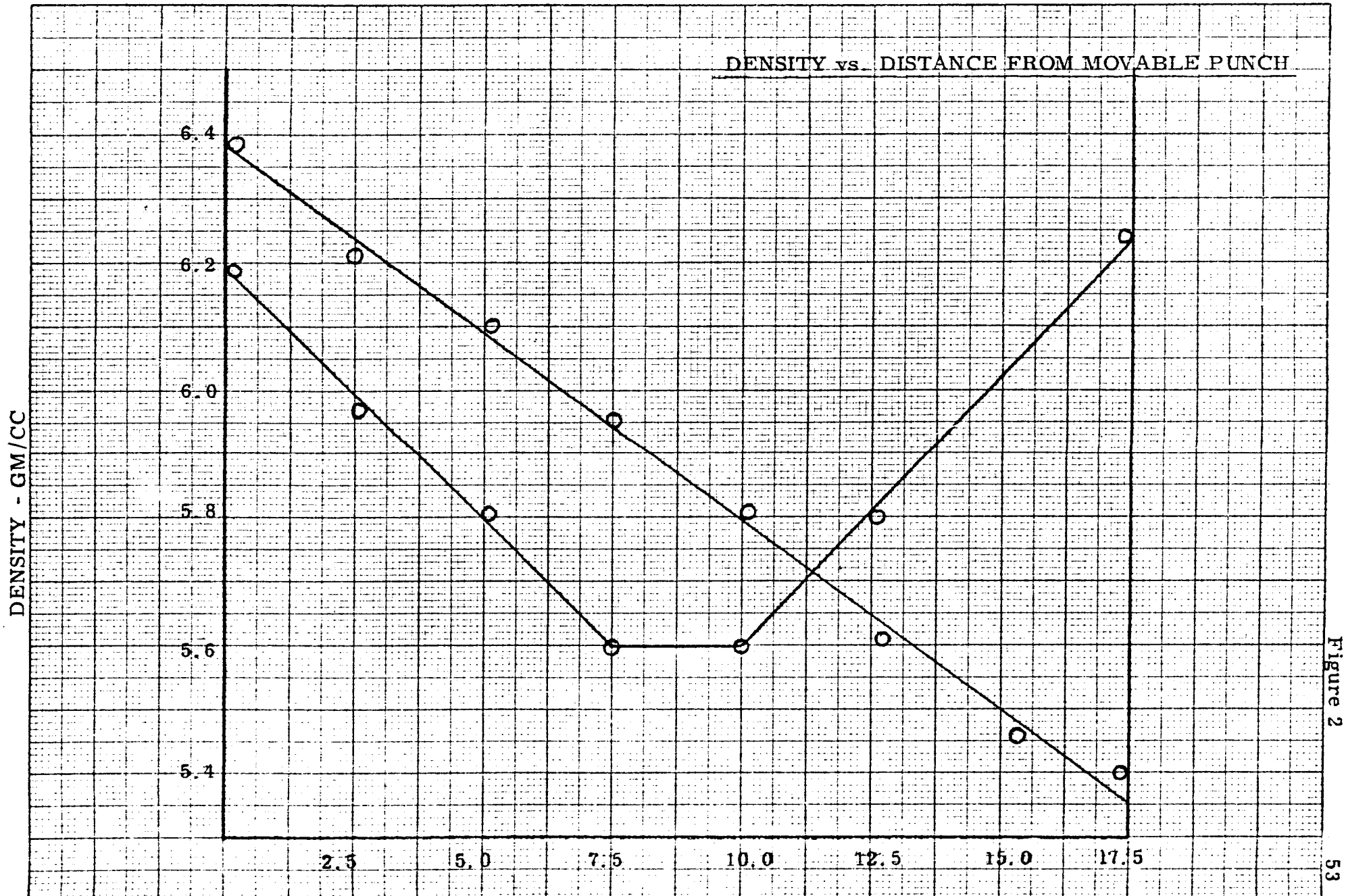

Figure 2

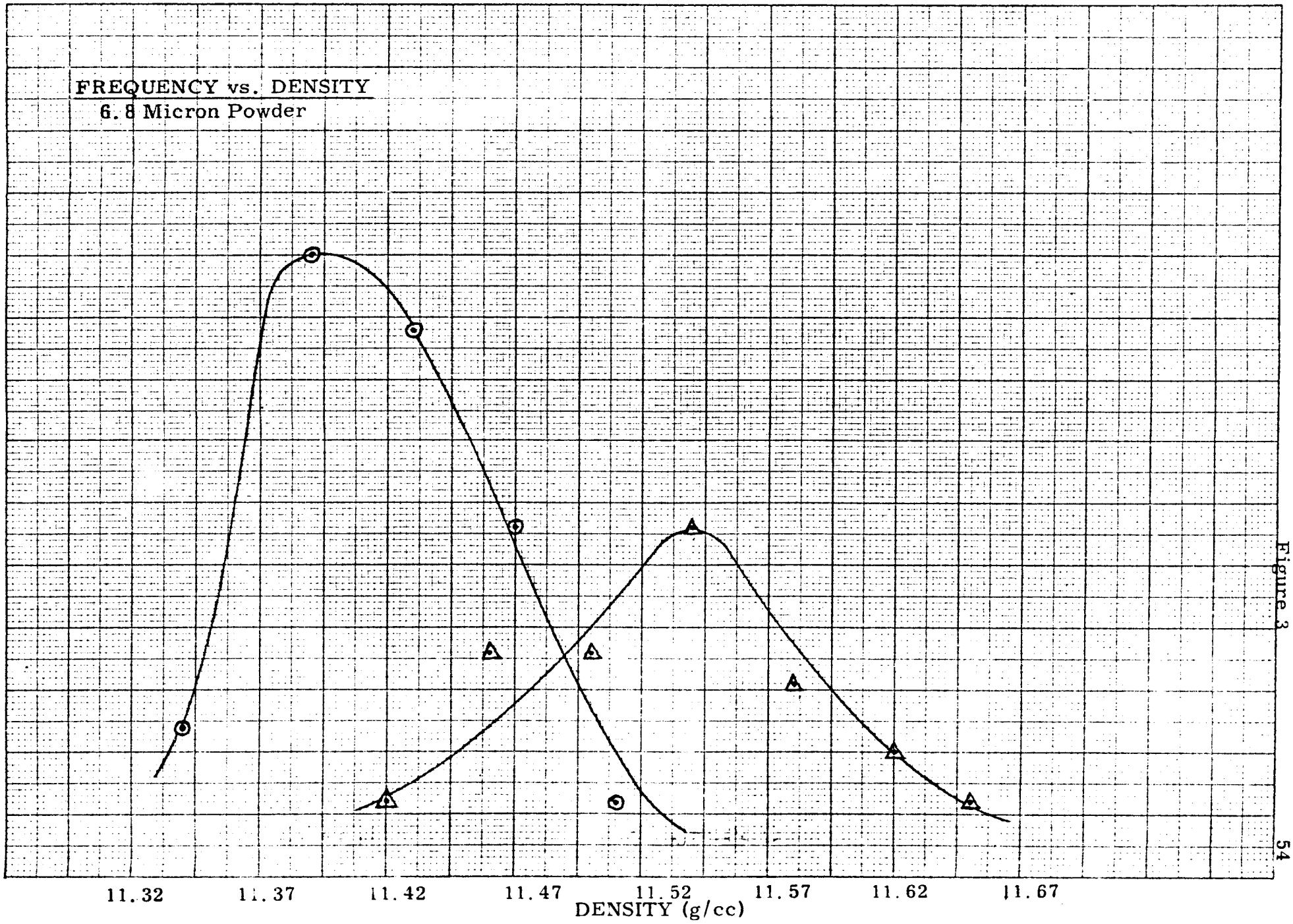
FREQUENCY vs. DENSITY
6.8 Micron Powder
30
25
20
15
10
5
11.32
11.37
11.42
11.47
11.52
11.57
11.62
11.67
DENSITY (g/cc)

Figure 3

Figure 4

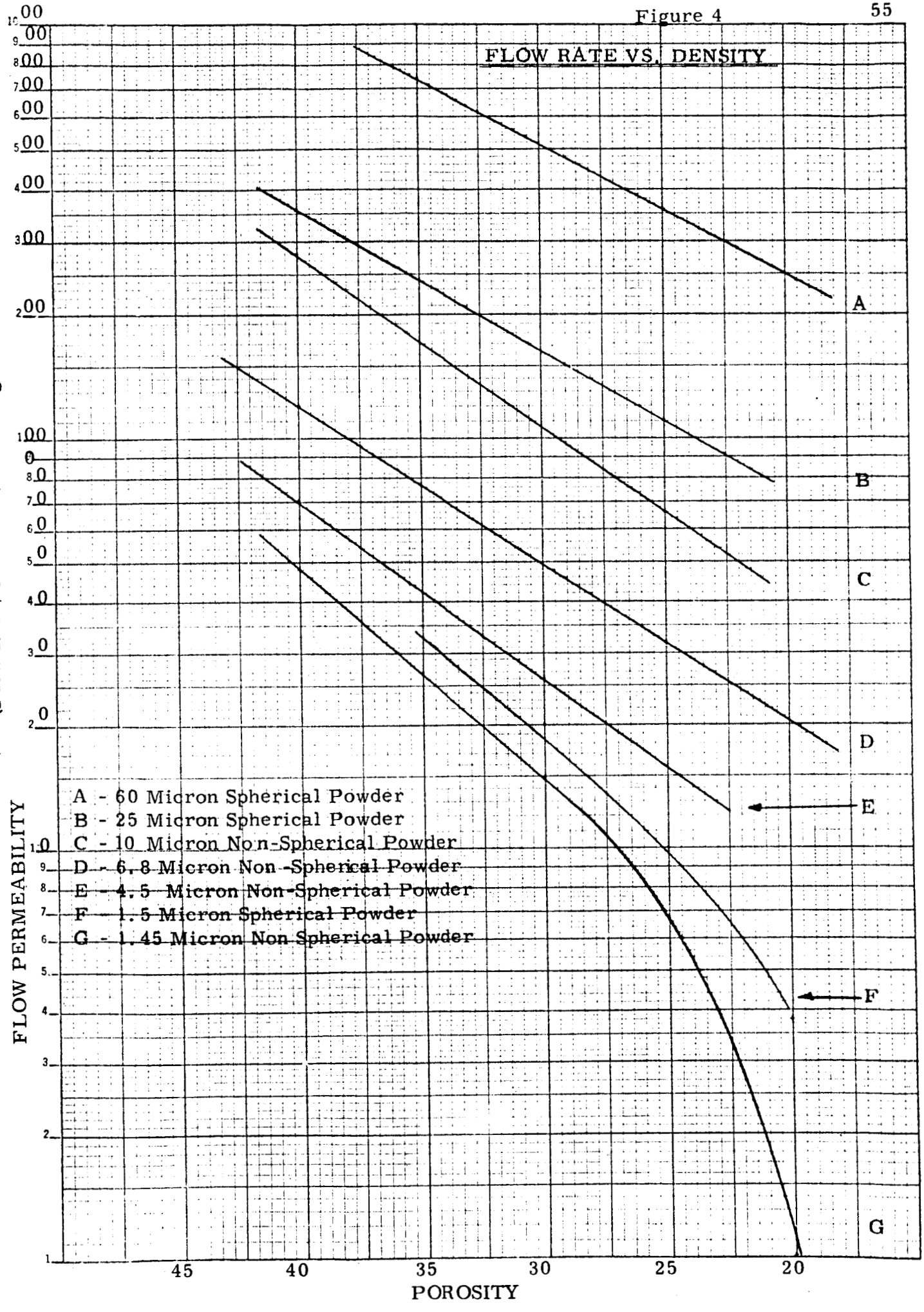
FLOW RATE VS. DENSITY
FLOW PERMEABILITY
(Flow Rate/Unit Area/Unit Length)
FLOW PERMEABILITY
POROSITY
45
40
35
30
25
20
A
B
C
D
E
F
G
A - 60 Micron Spherical Powder
B - 25 Micron Spherical Powder
C - 10 Micron Non-Spherical Powder
D - 6.8 Micron Non-Spherical Powder
E - 4.5 Micron Non-Spherical Powder
F - 1.5 Micron Spherical Powder
G - 1.45 Micron Non Spherical Powder

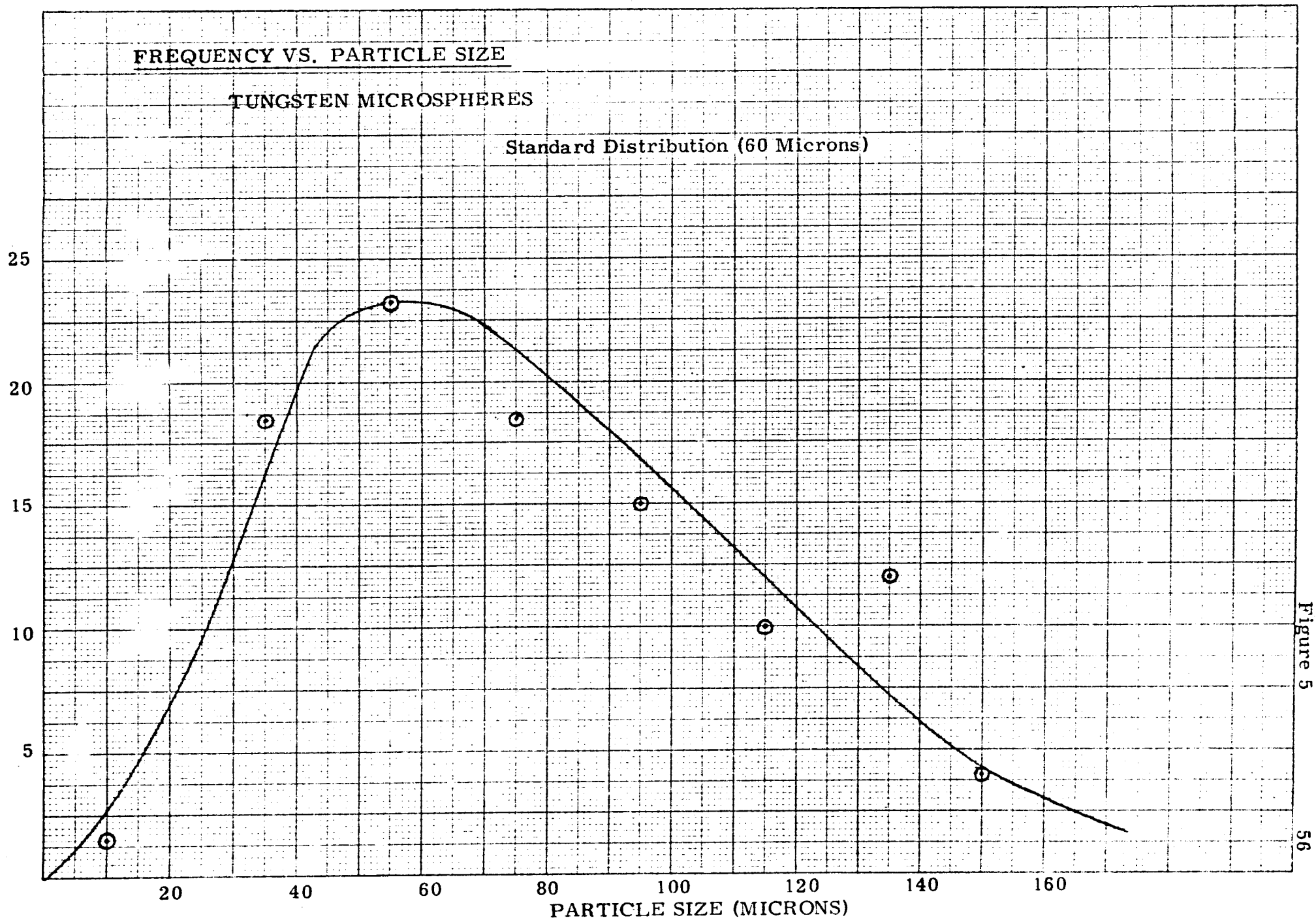
FREQUENCY VS. PARTICLE SIZE
TUNGSTEN MICROSPHERES
Standard Distribution (60 Microns)
25
20
15
10
5
20
40
60
80
100
120
140
160
PARTICLE SIZE (MICRONS)

Figure 5

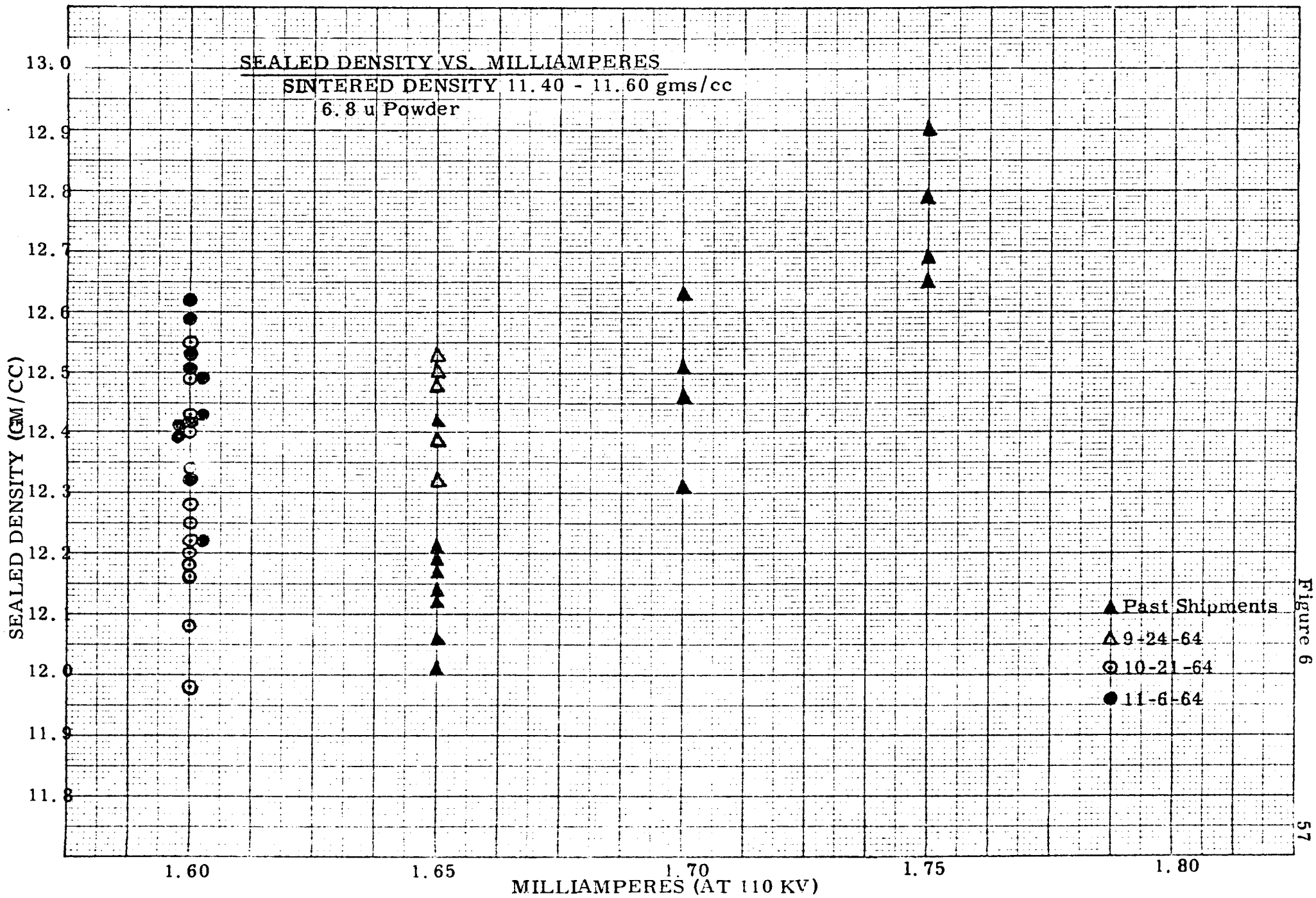
SEALED DENSITY VS. MILLIAMPERES
SINTERED DENSITY 11.40 - 11.60 gms/cc
6.8 u Powder
SEALED DENSITY (GM/CC)
13.0
12.9
12.8
12.7
12.6
12.5
12.4
12.3
12.2
12.
12.0
11.9
11.8
1.60
1.65
1.70
1.75
1.80
MILLIAMPERES (AT 110 KV)
Past Shipments
9-24-64
10-21-64
11-6-64

Figure 6

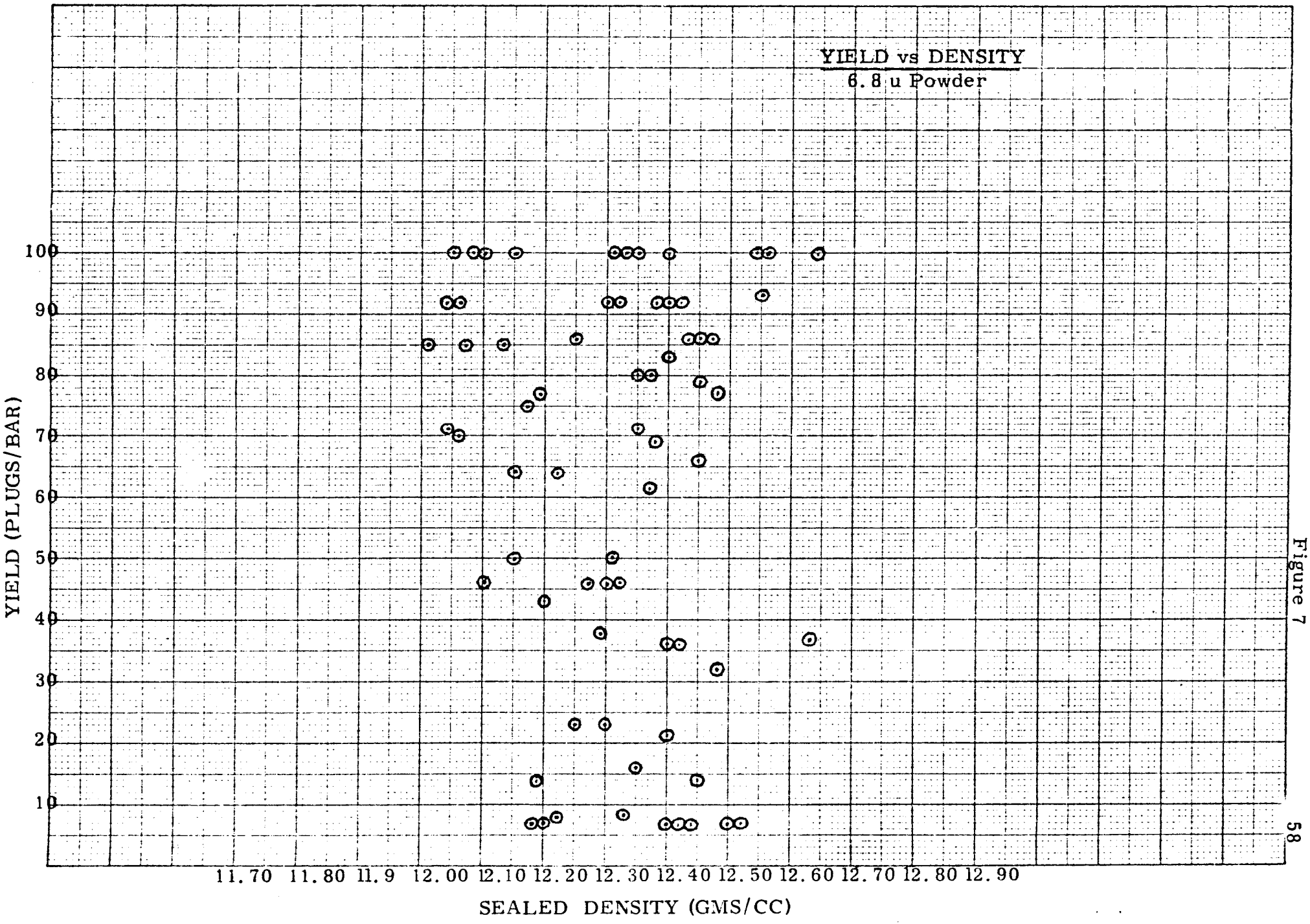

Figure 7

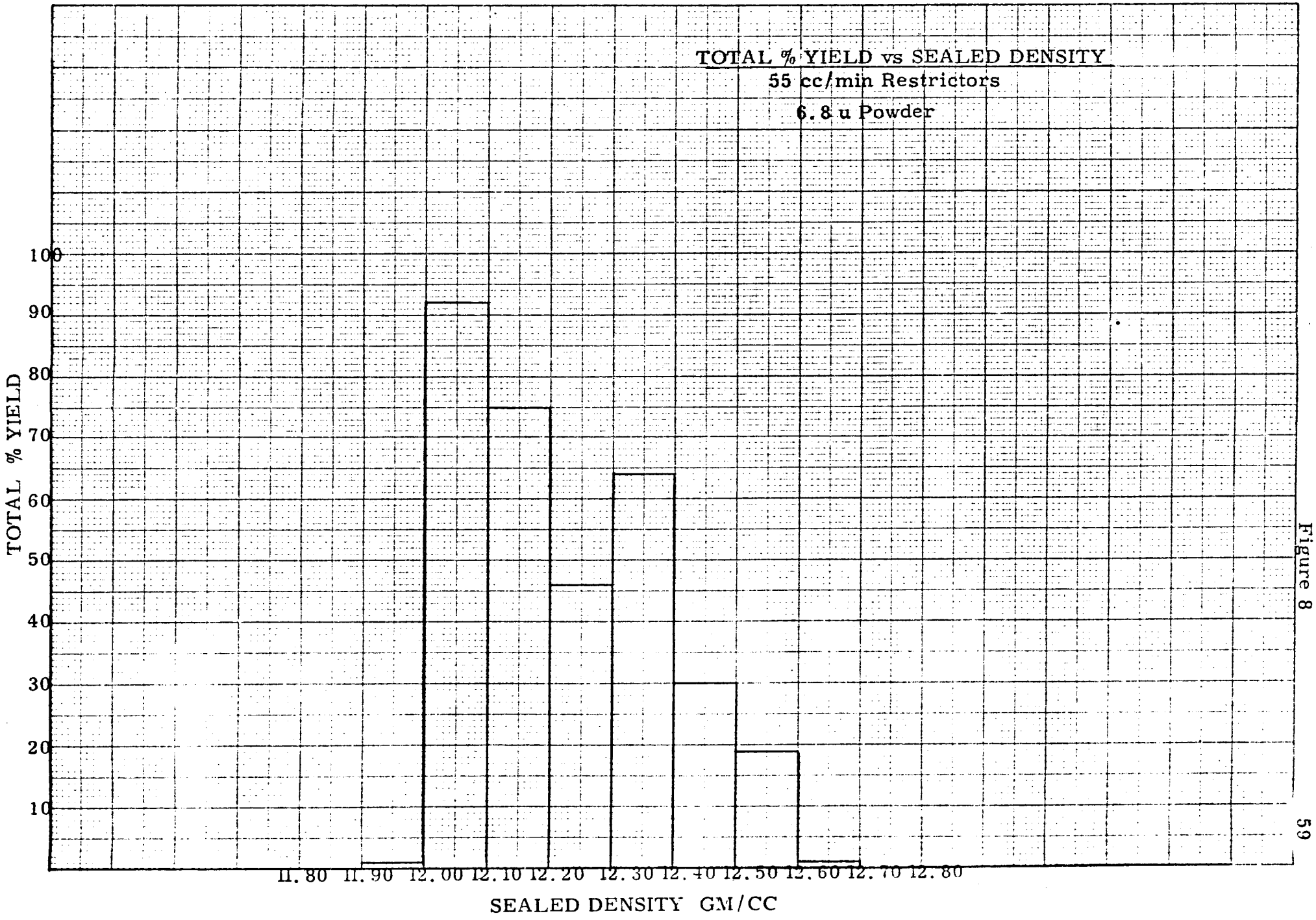

Figure 8

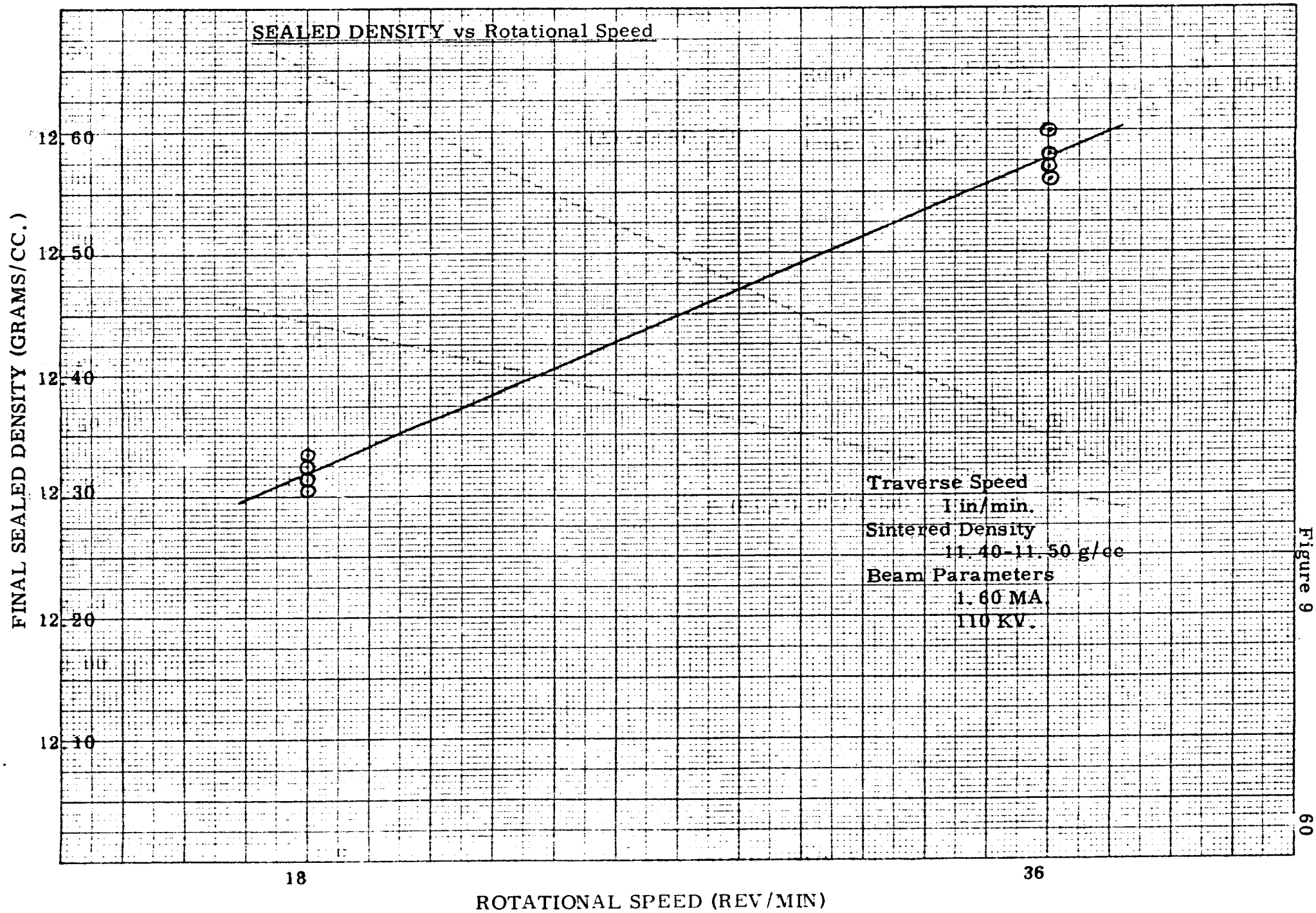

Figure 9

KEUFFEL & ESSER CO.

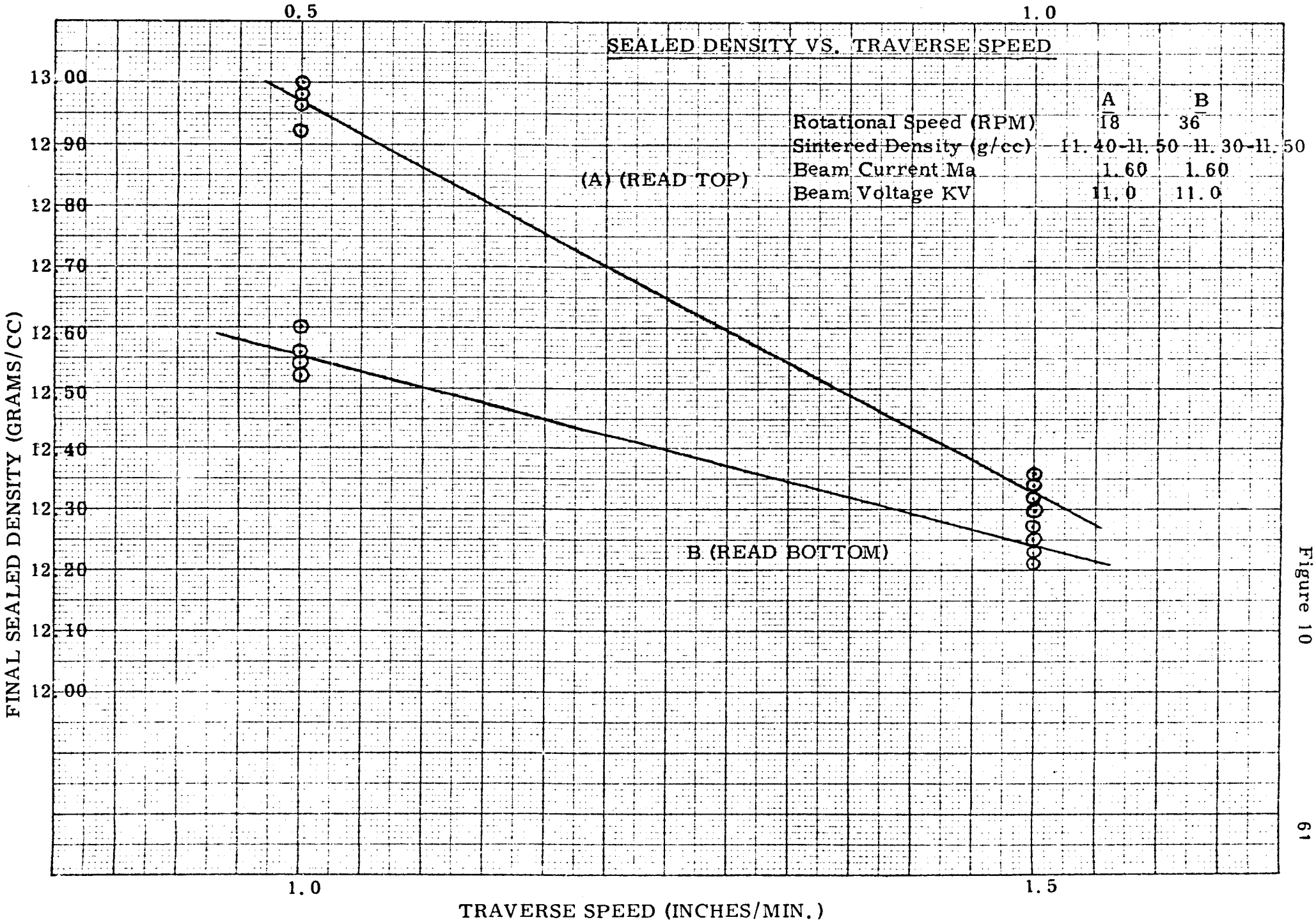

Figure 10

DRAWING

REVISIONS

SYM	WAS	DATE	BY	APP

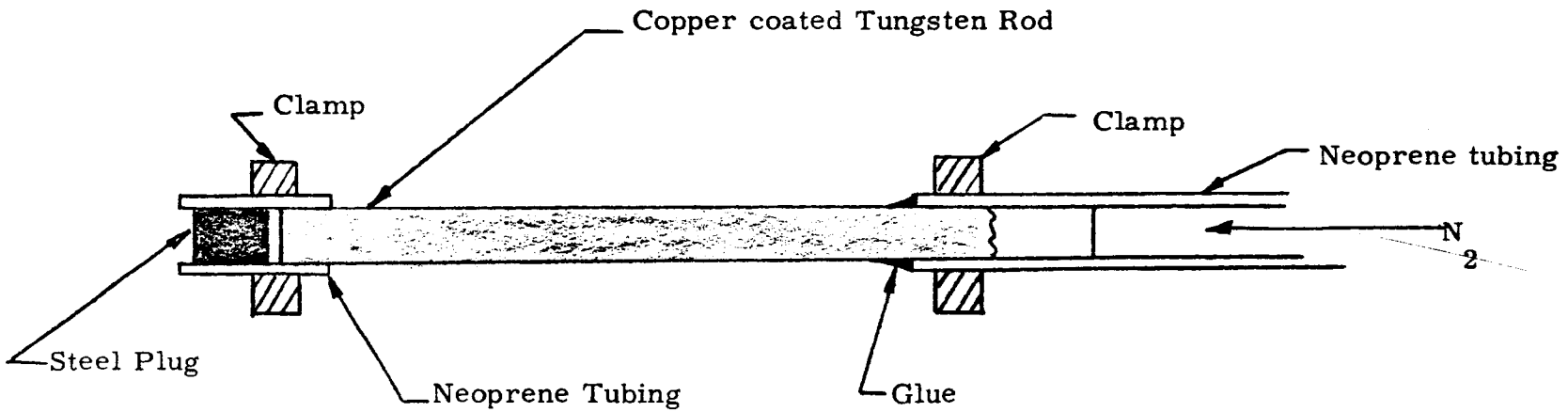

Figure 11

UNLESS OTHERWISE SPECIFIED, TOLERANCES ON FRACTIONS ± 1/64 ON DECIMALS ± .005		DESCRIPTION	MATERIAL	
DRAWN	CHECKED	LEAK TESTING DEVICE		KULITE TUNGSTEN CO. RIDGEFIELD, N. J.
DATE	SCALE			

62

OGILVIE PRESS, INC., BROOKLYN 17, N. Y. ULTRAVEL NO. 490M

Figure 12

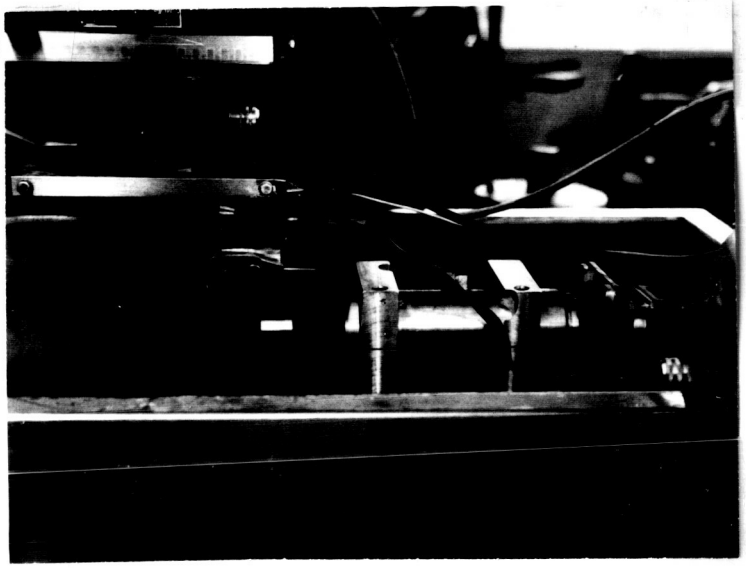

EDM fixture about to be immersed in oil prior to the actual cutting operation. In the foreground is a cylindrical graphite block which has four (4) grooves, 0.140" wide, for cutting the tungsten rod (directly behind graphite block). For every 1 part of the graphite cylinder this is eroded away, 8 parts of the tungsten rod are removed. Note the oil surrounding the assembly.

DRAWING

REVISIONS				
SYM	WAS	DATE	BY	APP

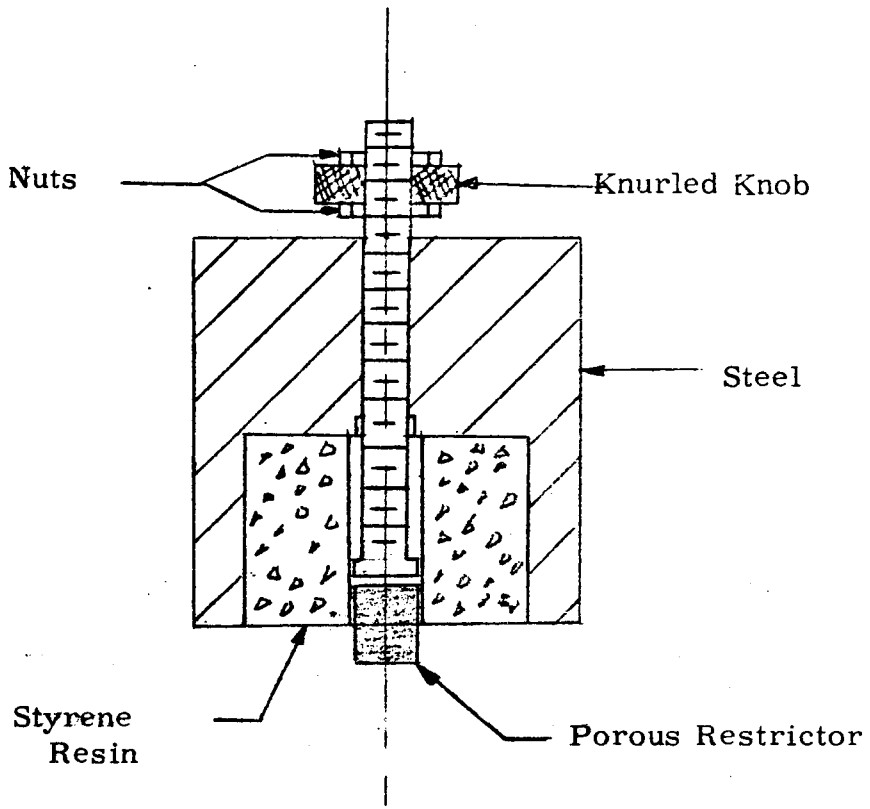

Figure 13

UNLESS OTHERWISE SPECIFIED, TOLERANCES ON FRACTIONS ± 1/64 ON DECIMALS ± .005		DESCRIPTION	MATERIAL	KULITE TUNGSTEN CO. 64
DRAWN	CHECKED			RIDGEFIELD, N. J.
DATE	SCALE	LAPPING FIXTURE		

OGILVIE PRESS, INC., BROOKLYN 17, N. Y. ULTRAVEL NO. 490M

Figure 14

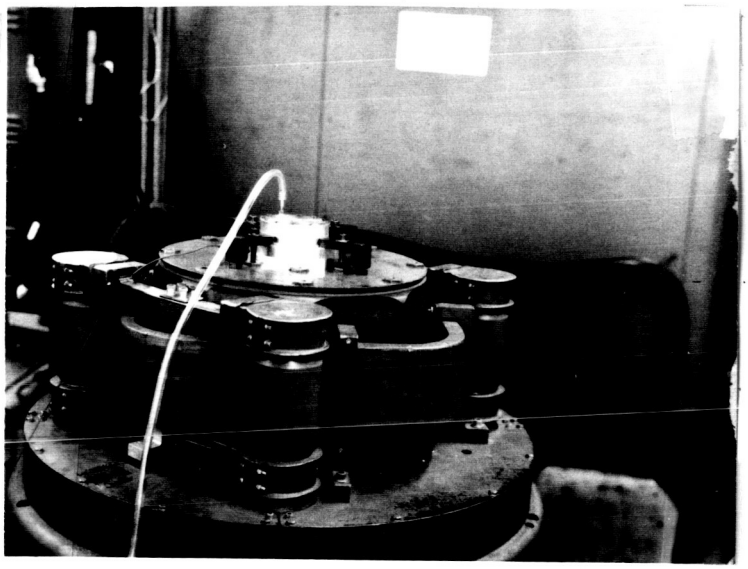

Vibration fixture mounted on top of a C25H Vibratory. Plastic tubing is for flow of nitrogen into fixture during the test.